Proceedings of the ASME 2010 3rd Joint US-European Fluids Engineering Summer Meeting and 8th International Conference on Nanochannels, Microchannels, and Minichannels
FEDSM-ICNMM2010
August 1-5, 2010, Montreal, Canada

FEDSM-ICNMM2010-30186

NUMERICAL SIMULATION AND COMPARSION OF PUMP AND PUMP AS TURBINE

Sun-sheng Yang
Research Center of Fluid Machinery Engineering and Technology
Jiangsu University, Zhenjiang, China
yangsunsheng@126.com

Fan-yu Kong
Research Center of Fluid Machinery Engineering and Technology
Jiangsu University, Zhenjiang, China
kongm@ujs.edu.cn

Fei-Shao
Research Center of Fluid Machinery Engineering and Technology
Jiangsu University, Zhenjiang, China
shaofei4535@163.com

Ting-Wang
Research Center of Fluid Machinery Engineering and Technology
Jiangsu University, Zhenjiang, China
arywang@126.com

Xiao-kai Shen
Research Center of Fluid Machinery Engineering and Technology
Jiangsu University, Zhenjiang, China
jxky009@126.com

ABSTRACT

A numerical comparison of a conventional pump in pump and pump as turbine (PAT) mode is presented. The numerical simulation is carried out with ANSYS CFX software by means of steady state analysis. Through CFD analysis, the relationship of two modes' performance characteristics, volumetric efficiency, axial thrust and flow field distribution and etc. were acquired. The possible direction for optimization of PAT is clear according to the PAT flow field distribution.

Keywords: CFD, pump, pump as turbine, comparison，flow field distribution

INTRODUCTION

With the increasing energy demands, improving the efficiency of energy generation and energy consumption is critical in the resolution of energy crisis. One of the cheap and attractive approaches in small waterpower resources recovery is using pumps in reverse operation as turbines. Pumps are readily made small machines, easy to maintain and mass-produced. Researchers have shown that PAT in small hydropower can compete with conventional turbines in respect to capital investment and efficiency.

However the characteristics of PAT are unknown in the design and selection process of appropriate pump. Many prediction methods have been developed in the prediction of PAT performance and selection of appropriate pump to be used as turbines [1-5]. However due to the complex nature and various type of pumps, none of the prediction method is absolutely reliable. With the development of computer technology, CFD provides a relatively reliable tool for the prediction, design and selection of appropriate pumps to be used as turbines.

Rotational fluid machinery is completely reversible and pumps can run efficiently as turbines. However, performances in both modes are not identical although the theory of ideal fluids would predict the same. In this paper, detailed comparisons are drawn between these two modes of operation. Through CFD analysis the difference between pump and PAT is clear, and possible direction for geometric optimization of PAT could be performed in future research work.

NOMENCLATURE

Q	pump volume flow rate, m^3/s;
n	rotational speed, r/min;
H	head, m;
$n_s = \dfrac{3.65n\sqrt{Q}}{H^{0.75}}$	specific speed;
q	leakage amount, m^3/s;

$Q_t = q + Q$ theoretical flow rate, m^3/s;

$\eta_v = \frac{q}{Q_t} \times 100\%$ volumetric efficiency;

β_{b1} inlet blade angle, (°);

β_{b2} outlet blade angle, (°);

β_1 inlet relative flow angle, (°);

β_2 outlet relative flow angle, (°);

α_1 inlet absolute flow angle, (°).

PUMP GEOMETRY

The focus of the investigation is a single stage end suction centrifugal pump with its specific speed of 69. Fig. 1 provides the internal flow field within the pump control volume. Table 1 lists the main geometric parameters of the pump. As is seen from Fig. 1, appropriate extension has been done in the inlet and outlet section.

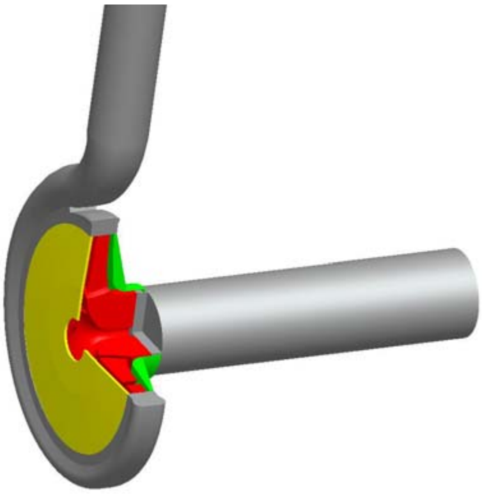

Figure1. Internal flow field within the pump control volume

Table 1. Main geometric parameters of pump

Description	Value
Inlet eye diameter	120 mm.
Blade type	Inlet twisted
Blade number	5
Blade wrap angle	125°
Pump outlet blade angle	38°
Blade thickness	5 mm
Impeller diameter	304 mm
Impeller outlet width	18 mm
Impeller ring length	25 mm
Clearance between impeller and casing wear ring	0.48 mm
Volute type	Spiral
Volute outlet diameter	80 mm
Base circle diameter	334 mm
Gap between impeller outlet and volute base circle diameter	30 mm

NUMERICAL MODEL AND COMPUTATIONAL METHODOLOGY

The pump rated operating point is flow rate $200m^3/h$, head 120m, rotational speed 3000r/min. When in PAT mode the rotational speed is the same as in pump mode.

Geometry and Grid

To simplify the model, the fluid in the pump front and back chamber is usually neglected in the CFD simulation. This simplification which only has a minor effect in pump performance, is reasonable in pump simulation, however it is not the same case for PAT. Relative large error has been reported in PAT mode [6,7], due to the importance of PAT inlet flow. In order to get a more accurate result all fluid in the pump control volume was modeled as is indicated in Fig. 1 in this paper. A structured hexahedral mesh was generated for each part. Fig.2 gives a general view of the mesh. A grid independence study was performed ranging from 0.5 to 1 million meshes, the variation of results was within 1%. The final number of meshes are listed in table 2.

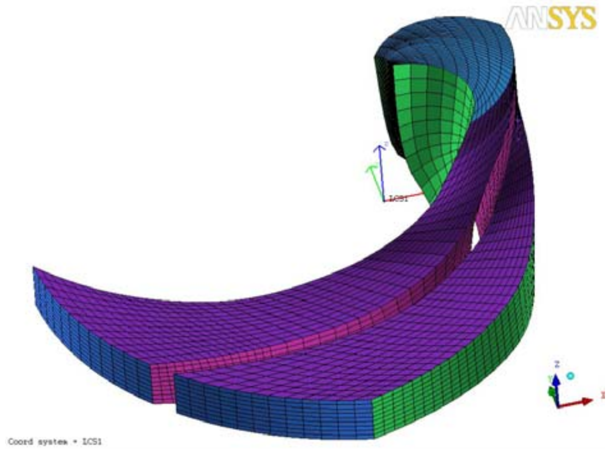

(a) Meshes in one impeller passageway

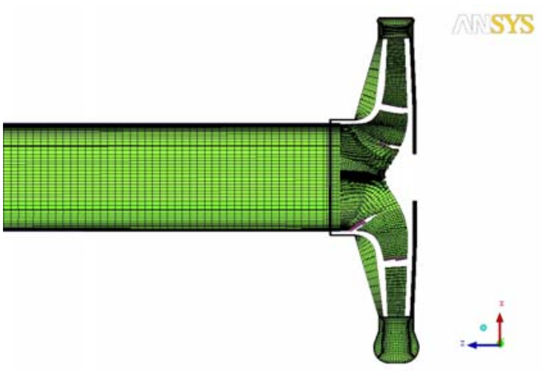

(b) Meshes in an axial cutplane

Figure 2. General view of meshes

Table 2 Number of meshes in each part

Suction inlet	Impeller	Front chamber	Back chamber	Volute	Total
88312	255240	84835	61628	275626	765641

Solution Parameters

The 3D steady Navier-Stokes equation was solved using finite-element based finite-volume method [8]. The turbulence was simulated with RNG k-ε turbulence model. The advection scheme was set to high resolution. And the convergence criterion is 10^{-5}.

As the motion of the impeller blades relative to the stationary volute is central to the investigation, the analysis must involve multiple frames of reference. The suction inlet and volute were set in stationery frame and the impeller was set in rotary frame. The interface between each part is set as follows.

Between two stationary components: general grid interface.

Between rotational and stationary components: rotor stator interface.

The inlet and outlet boundary conditions were set to total pressure inlet and mass flow outlet[9]. All the surface roughness within the control volume was set to 25μm.

All the calculations were performed on Dell Workstation T5500 which has eight 2.00GHz cores and 12.0GB memory. It took more than three days to accomplish all the calculations.

NUMERICAL ANALYSIS

Comparsion of performance characteristics

In general the best efficiency point (BEP) of turbine is higher than that of pump in flow and head. Many researchers have tried to find the relation between pump and PAT performance characteristics. However due to the complex nature and multiple types of pumps, none of the prediction is 100% reliable. Fig. 3 shows the performance characteristics of pump and PAT. It is to be pointed out that the mechnical efficiency is neglected in the calculation of efficiency.

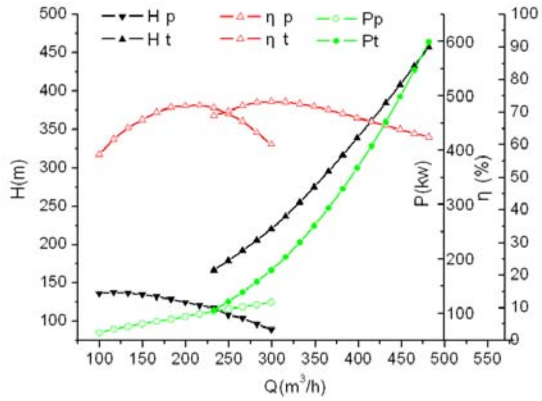

Figure3. Performance characteristics of standard pump in pump and PAT modes

As can be seen from Fig.3, the PAT output power and head increases with flow in the form of parabolic curve. The pump output power increases while the head decreases with increasing flow. The two modes best efficiency point's efficiency is almost the same. The flow rate and head at the best efficiency point of PAT is 1.56 and 1.77 times of that of pump mode respectively. The efficiency in turbine mode does not drop with increasing flow as rapidly as in pump mode.

COMPARISON OF VOLUMETRIC EFFICIENCY

A small amount of high pressure fluid in the volute side flows towards the pump suction pipe or PAT outlet pipe due to the pressure difference and forms the leakage loss. Besides additional hydraulic loss is inevitable due to the difference of the radial leakage flow direction and the axial flow direction in the pipe. In the design process, people usually try to reduce the leakage amount in order to improve the volumetric efficiency.

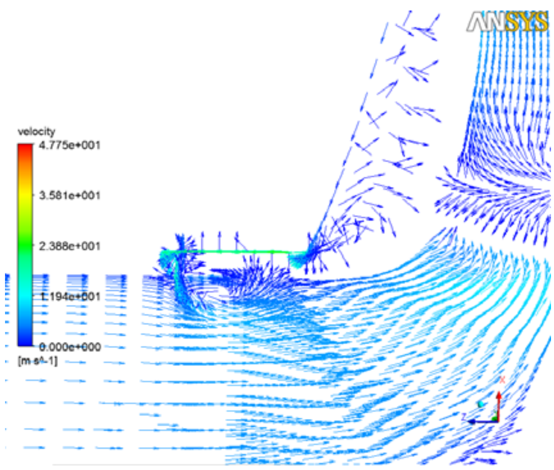

(a) pump leakage flow

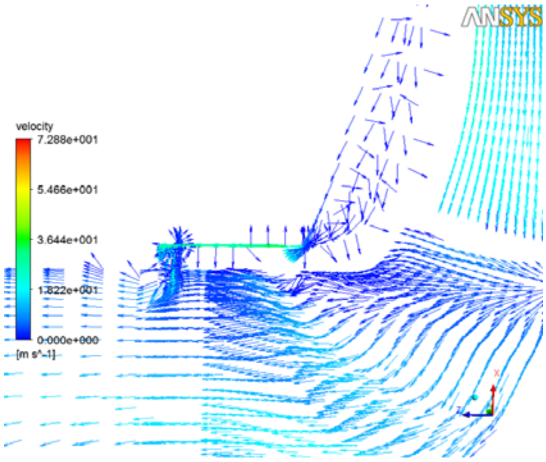

(b) PAT leakage flow

Figure4. Pump leakage flow in pump and turbine mode

The leakage amount of pump through the wear ring in two modes were acquired and plotted in Fig. 5. It is found that the leakage amount of pump is a little more than 14 m^3/h and varies little with flow. Due to the increase of flow, the volumetric efficiency ranges from 87.65% in part load to 95.76% in over load region. The reason for the nearly constant leakage amount at different operating conditions is that the pressure difference which caused the leakage is directly related to the impeller geometric parameters and rotational speed. We assume these parameters remain constant in this study. However, when in turbine mode, the pressure difference between volute inlet and impeller outlet increases with the increase of flow capacity, thus causing the leakage amount to increase with increasing flow. The volumetric efficiency in PAT ranges from 93.37% to 95.63% as can be seen in Fig 5.

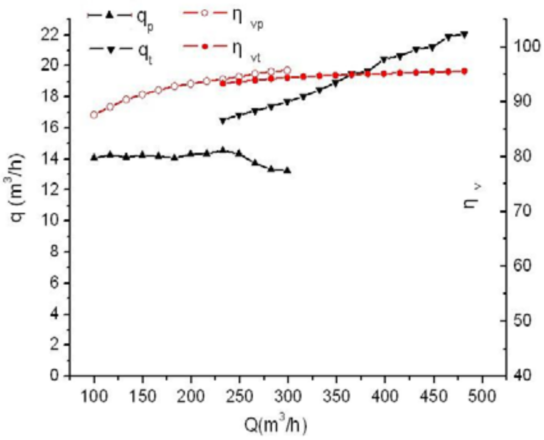

Figure5. Comparison of pump and PAT leakage amount

Comparison of Axial Thrust

The axial thrust is caused by the asymmetry of front and back cover, dynamic reaction force as flow direction changes from axial to radial, the unbalance pressure distribution at the two shaft ends and the weight of rotating elements etc.. In this paper only axial thrust caused by asymmetry of front and back cover is considered. Fig. 6 shows the axial thrust of standard pump in pump and turbine mode. The axial thrust in pump mode varies little in the scope of 10~13 kN in the operating range while the axial thrust in turbine mode increase nearly lineraly with the increase of flow.

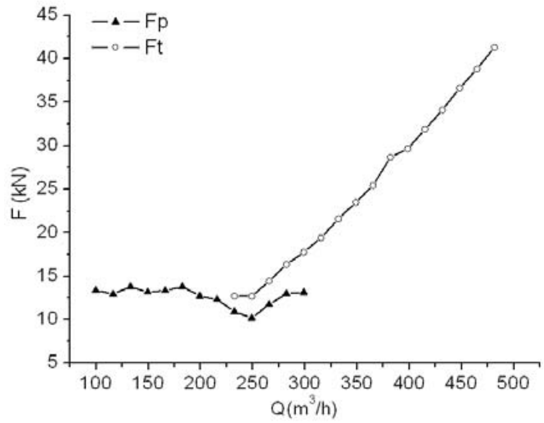

Figure 6. Comparison of axial thrust in pump and turbine modes

Comparison of Pressure Field Distribution in Impeller and Volute

Pump and PAT static pressure distribution through mid-span (XY plane of Fig. 1) of impeller and volute is presented in Fig.7 and Fig.8 respectively. It is observed in Fig. 7 that the pressure in the outlet section of volute gradually decreases with increasing flow, which is in accordance with the fact that the head diminishes with the increase of flow. Also it is observed that the pressure in the semi-enclosed spiral zone may exceed that in the outlet enclosed zone in the overload region.

Fig. 8 shows that the pressure in the PAT volute inlet region varies little with flow. This is because total pressure inlet boundary condition which assumes the inlet total pressure remains constant is applied. The static pressure diminishes along each passageway from the outer periphery to the impeller outlet section. As flow rate is increasing, there is a more pronounced variation of the pressure along the volute, and the magnitude of the static pressure at the inlet of impeller is also increased. This increase in pressure causes the impeller to get more energy from the fluid, and thus the increase of output power. This could help explain why the head of PAT in head versus flow curve increases with the increase of flow capacity.

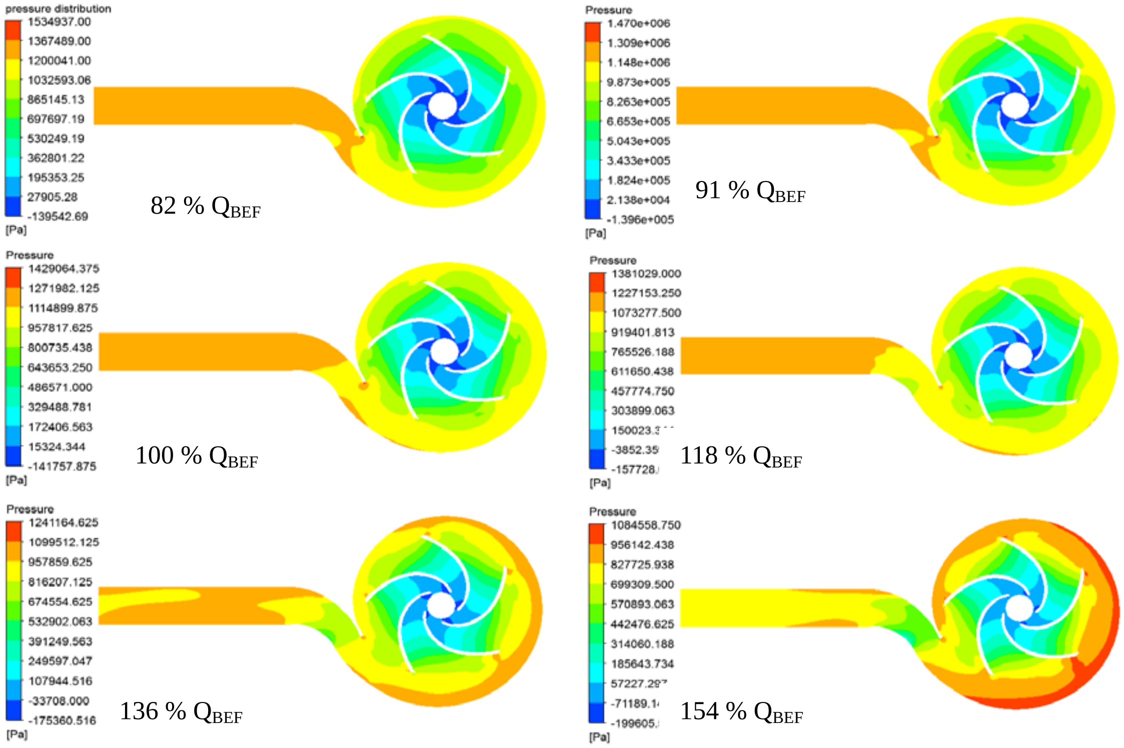

Figure7. Static pressure distribution in pump impeller and volute

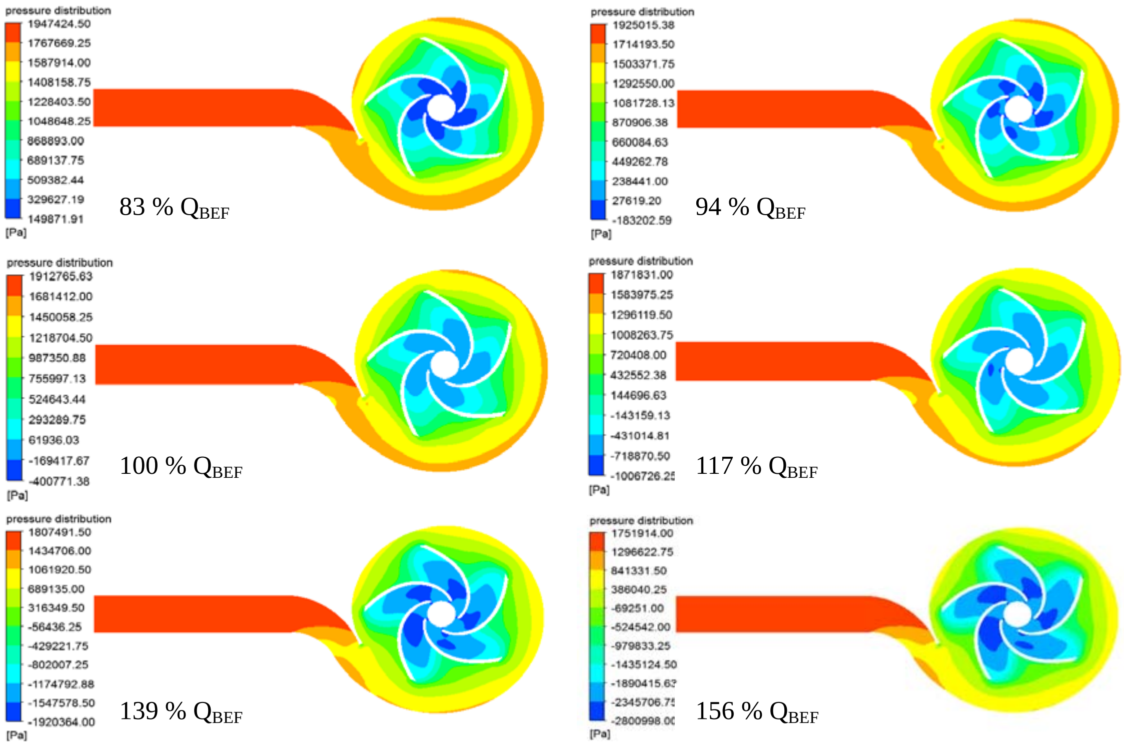

Figure8. Static pressure distribution in PAT impeller and volute

Comparison of Velocity Field Distribution in Impeller and Volute

In pump mode, the energy transformation between the fluid and the impeller is mainly determined by the shape of the vanes at the impeller outlet. The volute performs the function of gathering high velocity fluid from impeller and transforms the velocity energy into pressure energy to reduce the energy loss caused by high velocity fluid.

Fig.9 shows the velocity distribution in pump mid-span through volute and impeller. As is demonstrated in Fig. 9, pump flow field distribution in each flow passage is not identical at partload and overload region. The tendency of relatively high velocity fluid in the impeller suction side becomes apparent with the increase of flow capacity. A small swirl which rotates in the opposite direction of each passageway could be observed regardless of the capacity. Possible increase of numbers of impeller vanes or splitter vanes could improve the flow field

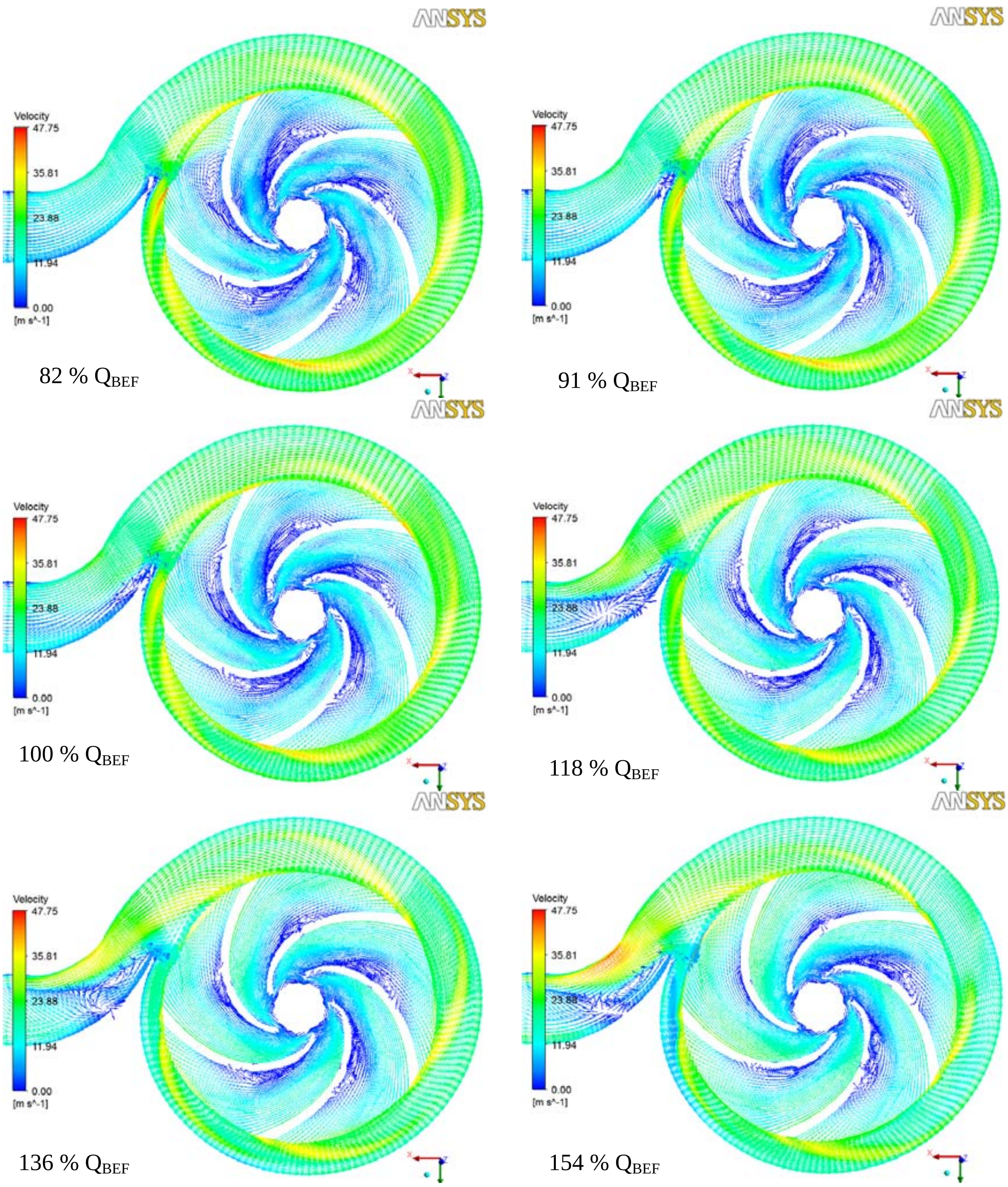

Figure9. Velocity distribution in pump impeller and volute

distribution in impeller passage. Also jet-wake phenomena caused by impeller vanes are clearly observed in the volute inlet region.

Fig.10 shows the velocity field distribution in PAT impeller and volute. As is indicated in Fig.10 two vortex regions A and B are formed in each impeller passage. The swirl direction of each region is in reverse of the impeller rotational direction. The area and intensity of vortex region A is enlarging while that of vortex region B is decreasing with increasing flow. This enlarging of swirl area together with that of the enlarging hydraulic loss due to the increase of flow capacity causes the efficiency drop of the PAT after the best efficiency point.

Unlike conventional turbine, PAT has no guide vane system. When flow is reversed in turbine mode, the volute guides the high energy fluid to the impeller flow passage. The volute provides a symmetrical flow and a certain amount of velocity momentum to each impeller passageway. The absolute

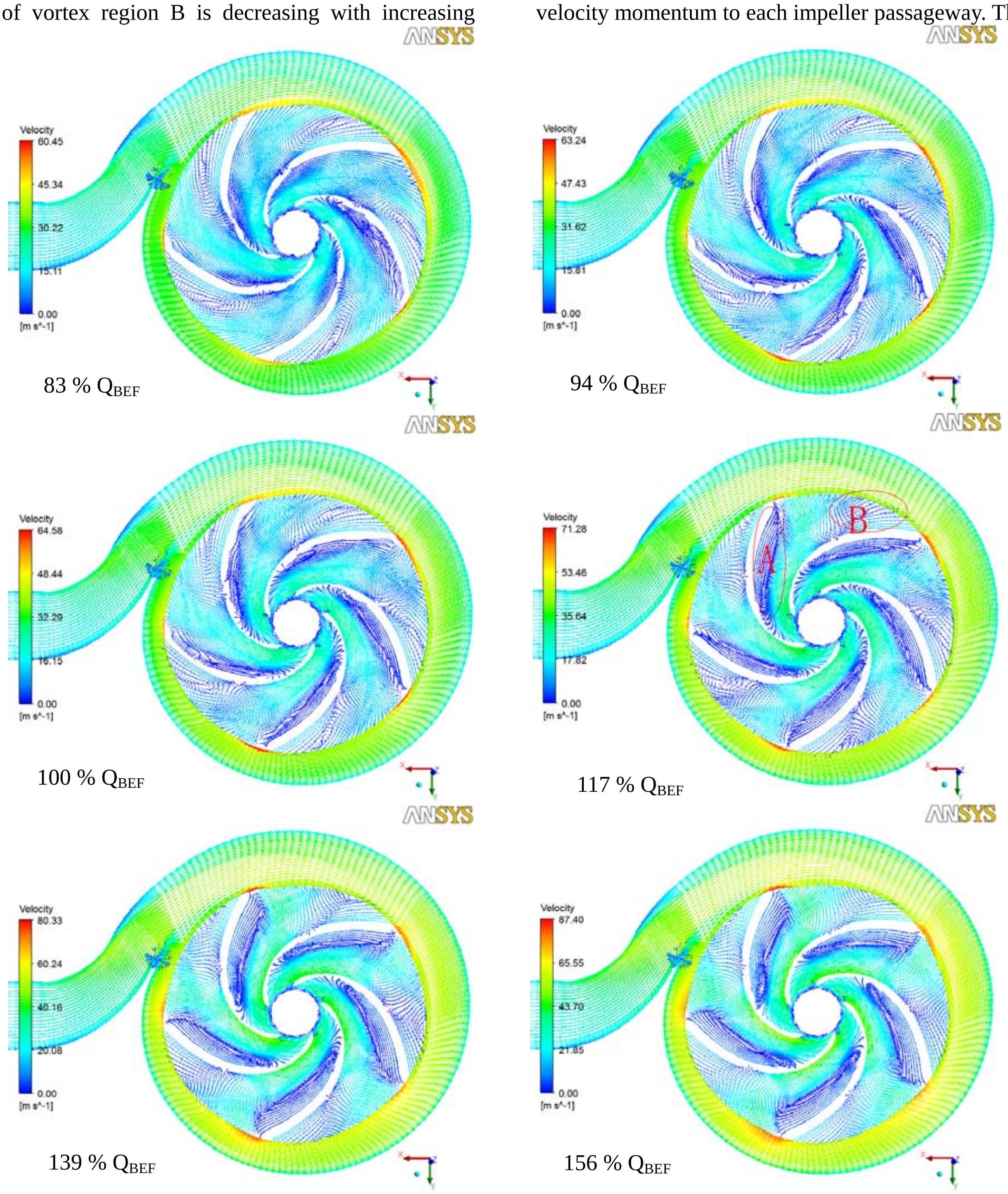

Figure10. Velocity field distribution in PAT impeller and volute

inlet angle remains constant at various flow. As is indicated in Fig.11, there is a rise of the relative flow angle β_1 with the increase of meridional velocity c_m caused by increasing flow rate. The PAT inlet attack angle $\alpha = \beta_1 - \beta_b$. The PAT inlet blade angle β_b is fixed in the operating range. So the inlet attack angle enlarges with increasing flow. This helps explain why the swirl region A which is caused by inlet attack angle increases with increasing flow. As is seen from the velocity field distribution, there is a small inlet attack angle even at the part load point and this attack angle increases with flow. So in order to improve the efficiency of PAT, possible increase of absolute fluid angle α_1 or the impeller vane angle β_b is indispensible for reducing the shock loss caused by inlet attack angle. As for the B swirl area, which may be caused by finite number of impeller vanes, possible increasment of impeller vanes or splitter vanes could diminish it. The detailed relation of the volute and impeller vane geometry to the performance of PAT is the object of our next stage research work.

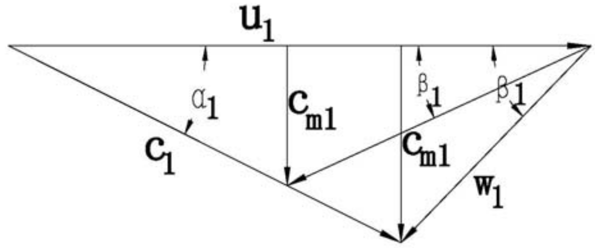

Figure11. PAT inlet velocity triangular angle

Comparison of tangential flow in the Pump inlet pipe

To visualize the tangential flow in the pump inlet pipe or PAT outlet pipe, the tangential velocity was projected on a radial cutplane 20 mm away from the rotating impeller. Fig. 12 shows the pump tangential velocity distribution in the cutplane. As is indicated in Fig.12 the tangential component caused by the rotation of the impeller rotates in the same direction of the impeller in the partload region and the tangential component diminishes at best efficiency and overload region.

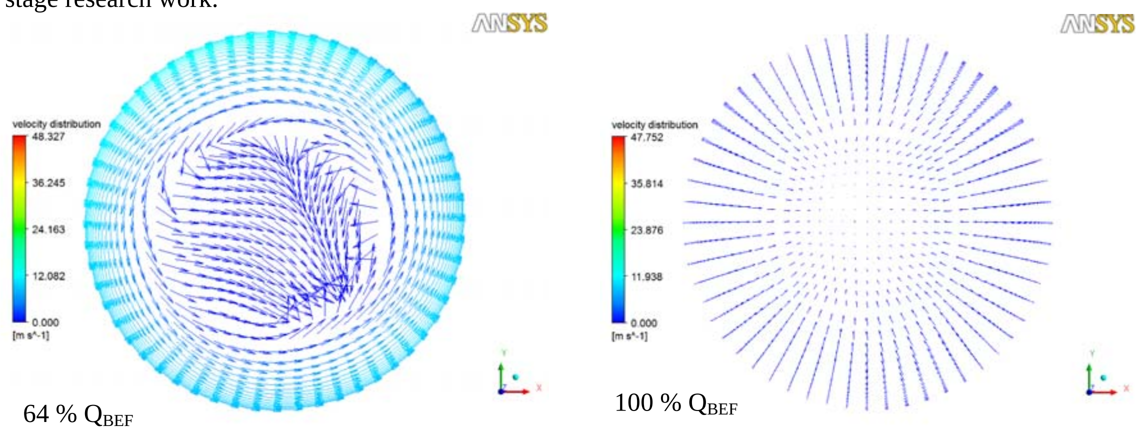

Figure12. The tangential component distribution in pump inlet pipe

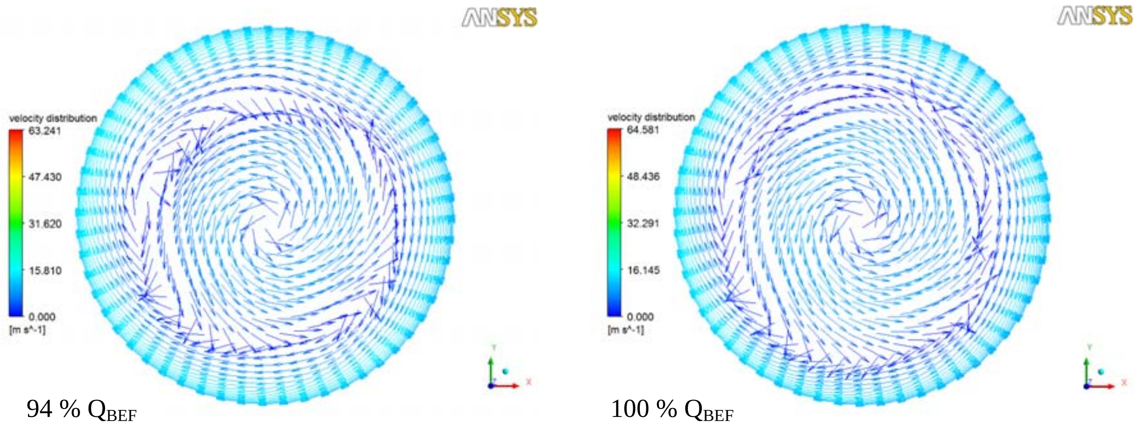

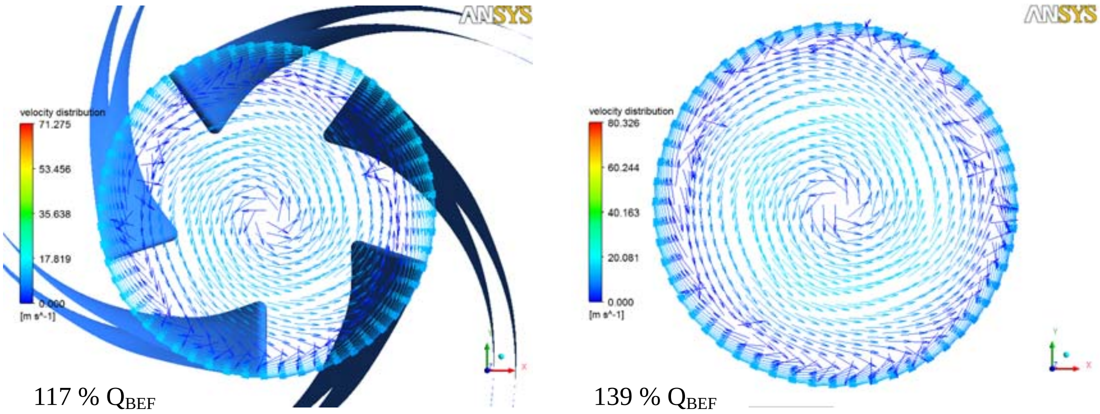

117 % Q_{BEF} 139 % Q_{BEF}

Figure13. The tangential component distribution in PAT outlet pipe

Fig.13 shows that the velocity of tangential component rotates in the reverse direction in the middle and out peripheral of the cutplane. And the area of the inner rotating velocity component is enlarging with increasing flow. The tangential component in the out peripheral caused by the rotation of impeller shroud rotates in the same direction of the impeller. The tangential component of inner area determined by impeller outlet angle β_{b2} as is indicated in the lower left picture of Fig.13 rotates in the opposite direction of the impeller. This hydraulic loss caused by swirl component together with the pipe friction loss forms the hydraulic loss in the PAT outlet pipe. Possible optimization of the PAT outlet blade angle and PAT outlet pipe shape could reduce this hydraulic loss.

CONCLUSION

The performance of a conventional centrifugal pump running in pump and turbine mode was numerically investigated by means of software ANSYS CFX. This work was carried out with full steady 3D-flow simulations. The purpose of the investigation was to compare the main differences when standard pump is running in the two different modes using CFD.

The comparison between the two modes outer performance curves shows that the best efficiency of two modes is almost the same. The flow rate and head at the best efficiency point of PAT is 1.56 and 1.77 times that of the pump respectively. Unlike pump characteristics, the PAT's head and power increases with the increase of flow rate.

Through the investigation of leakage rate in the wear ring, it is revealed that the leakage rate varies little in pump operating range, while it increases with increasing flow in turbine mode. And the volumetric efficiency increases with increasing flow in both modes.

The axial thrust caused by the asymmetry of front and back cover varies little in pump mode, while in turbine mode it increases with the increase of flow rate.

Through the analysis of the two modes' pressure field distribution the energy transmission mechanism within the pump and PAT is clear. Two vortex regions caused by inlet attack angle and finite number of blades were discovered through the turbine impeller velocity field distribution. An interesting phenomena observed in PAT outlet pipe is that the tangential velocity component caused by the outlet blade angle and rotating shroud circulates in the opposite direction in the outlet pipe. And the tangential component caused by blade angle increases with increasing flow rate. Through the analysis of pump and PAT, the two modes' main differences are clear, and possible direction for optimization is revealed.

ACKNOWLEDGMENTS

The author would gratefully acknowledge the financial support of the national project entitled "The exploitation and utilization of hydraulic power recovery turbine". Special thanks also go to the reviewer and my co-authors who help me to finish this paper.

REFERENCES

[1]M. Amelio, S. Barbarelli, 2004, A One-Dimensional Numerical Model for Calculating the Efficiency of Pumps as Turbines for Implication in Micro-hydro Power Plants, In Procedings of ESDA：7th Bienial ASME conference Engineering systems Design and Analysis. July 19-22,2004 Manchester, UK.

[2]P.Singh,F.Nestman,An optimization routine on a prediction and selection model for the turbine operation of centrifugal pumps, Experimental Thermal and Fluid Science(2009), doi:10.1016/j.espthermflusci.2009.10.004

[3]S.Derakhsham.,A. Nourbakhsh, Theoretical, numerical and experimental investigation of centrifugal pumps in reverse operation. Journal of Experimental Thermal and Fluid Science 32(2008) 1620-1627

[4]S.Derakhsham., A. Nourbakhsh, Experimental study of characteristic curves of centrifugal pumps working as turbines in different specific speeds, Elsevier Journal of Experimental Thermal and Fluid Science 32(2008) 800-007

[5]Williams,A.A.,1994, The turbine performance of centrifugal pumps: a comparison of prediction methods Proc.Instn Mech.Engrs,vol.208,Pt ,A,pp.59-66.

[6]P.Singh, Optimization of the Internal Hydraulics and of System Design for PUMPS AS TURBINES with Field Implementation and Evaluation, Ph.D. Thesis. University of Karlsruhe,Germany,2005.

[7]R.G.Simpson, A.A.Williams, Application of computational fluid dynamcs to the design of pico propeller turbines，in: Proceedings of the International Conference on Renewable ENERGY for Developing Countires,2006.

[8]Help Navigator, ANSYS CFX, Release 12.0 ANSYS CFX-Solver Modeling Guide.

[9]Spence P, Amaral-Teixeira J, Investigation into pressure pulsations in a centrifugal pump…, Computer Fluids (2007), doi:10.1016/j. compfluid.2007.10.001